

# The Scanning Vibrating Needle Curemeter

## Problem presented by

Bryan Willoughby

*RAPRA Technology Ltd*

## Problem statement

The vibrating needle curemeter is a commercial device which continuously monitors material cure right through from the liquid to the solid phase in liquid curing systems for rubbers, plastics, paints and resins. It provides a continuous record of the development of viscosity and stiffness. The amplitude attenuation of a vibrating needle at resonance frequencies is the basic mechanism whereby the monitoring of the progress of a given cure is achieved. The Study Group was asked to develop a clearer understanding of the underlying success of the curemeter and via that understanding to assess the prospects of further utilization of the curemeter in evaluating rheological properties of a given cure.

## Study Group contributors

D. J. Allwright (Smith Institute)

C. J. Budd (University of Bath)

J. S. Byatt-Smith (University of Edinburgh)

A. D. Fitt (University of Southampton)

N. D. Fowkes (University of Western Australia)

J. Gravesen (Technical University of Denmark)

P. D. Howell (University of Nottingham)

S. D. Howison (University of Oxford)

J. R. King (University of Nottingham)

A. A. Lacey (Heriot-Watt University)

J. R. Ockendon (University of Oxford)

K. Parrott (University of Greenwich)

G. Richardson (University of Nottingham)

C. Wang (Lancaster University)

S. Wilson (University of Manchester)

## Report prepared by

D. J. Allwright

# 1 Introduction

The operation of the Scanning Vibrating Needle Curemeter (SVNC) and the areas where the Study Group ESGI2001 were asked to take things forward are summarized in the document [1] issued at the Study Group. We recall that the basic method of operation of the SVNC is that a carbon fibre needle is vibrated vertically in a sample as it cures, *i.e.* as it reacts and sets from a liquid to a solid. The sample is contained in a saucer-shaped depression in a steel base, roughly as illustrated in Figure 1. The vibration is driven

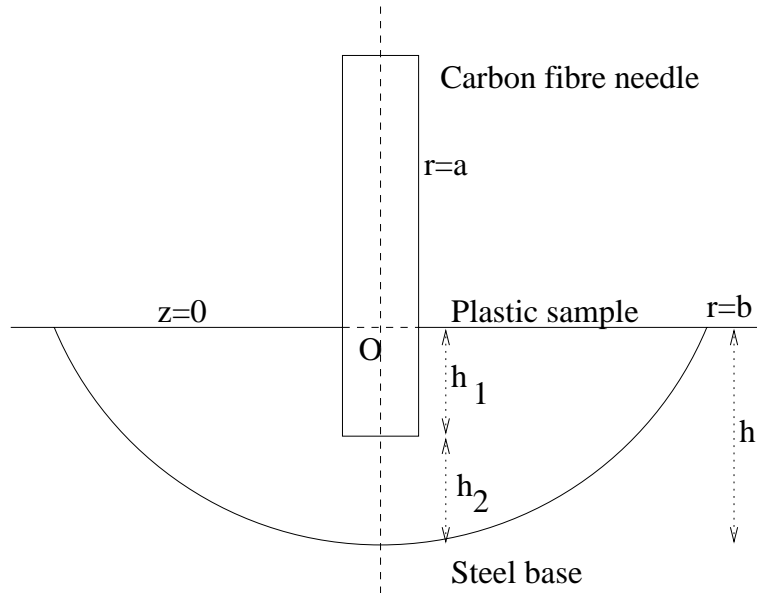


Figure 1: Basic sample geometry

electrically, by a constant thrust vibrator, at an adjustable frequency. The back emf (electromotive force) in the vibrator coil gives a measure of vibration amplitude, and the vibration frequency is computer-controlled to maintain the maximum amplitude. Thus during the cure, both the resonant frequency and the resonant amplitude are measured. In a cure that RAPRA provided details of, the resonant frequency rose from about 75 Hz to 170 Hz during the cure. RAPRA Technology can already gain much qualitative information from this curemeter. A brief note has been written previously on the quantitative aspects, [2], and the aim of the Study Group was to make further progress in this direction.

## 2 Modelling assumptions

There are various potential sources of nonlinearity in this problem, and the Study Group did not make any attempt to model them, but we do just list them here for reference:

- Sliding friction in the driving mechanism of the vibrator.
- Conversion of physical amplitude to output signal. The electronic processing that produces the signal intended to be proportional to back emf is not known in detail,

but it is intended to be linear.

- Non-Newtonian behaviour in the polymer.
- Imperfect bonding of the sample to the needle or the base.
- Partial buckling of the needle during the compressive phase of the cycle.

One piece of evidence of nonlinearity is that Bryan Willoughby (henceforth BW) has seen traces of the back emf as a function of time, and they were noticeably non-sinusoidal, whereas the driving force is sinusoidal. The reason for this is unknown.

Based on information provided by BW, we assume that

- the vibration does not affect the curing process, so the sample remains homogeneous and isotropic;
- the sample bonds perfectly to the needle and the base.

The base in which the sample sits is of steel, with Young's modulus about  $2 \times 10^{11}$  N/m<sup>2</sup>, and the Young's modulus of the carbon fibre needle is similar. However, the Young's modulus of the plastic sample when fully cured will be much lower, typically of order  $10^6$  N/m<sup>2</sup>. When the sample is liquid we shall see that the stiffness is lower. This suggests the basic approximation of treating the base and needle as rigid, so that the sample itself is the only deforming element in the system.

A further approximation is to treat the sample as incompressible. This is a natural assumption when the sample is still liquid. For the solid this assumption rests on two facts:

- the Lamé moduli  $\lambda$  and  $\mu$  satisfy  $\lambda \gg \mu$ ;
- there is a free surface so the material can accommodate the needle vibration without change of volume.

The first point here is certainly a good approximation for rubbers, and we believe it applies to plastics also, but do not have access to data from which to check it. It implies that Poisson's ratio  $\nu = \lambda/(2(\lambda + \mu))$  is close to  $\frac{1}{2}$ . Also the usual relation  $E = 2G(1 + \nu)$  between Young's modulus  $E$  and the shear modulus  $G$  ( $G = \mu$ ), becomes simply  $E = 3G$ . The second point is that since the bulk modulus is much larger than the shear modulus, and the geometry is such that the constraints can be satisfied by shear without volume change, that is what the material will choose to do.

### 3 Linear model

We shall describe a linear mathematical model for the vibration of the needle in the sample in the curemeter. We begin by describing the coordinates and variables we use, and then assemble together standard models for the different parts of the system.

### 3.1 Coordinates and variables

We choose a cylindrical coordinate system  $(r, \theta, z)$  based on the vertical axis of symmetry, with origin at the centre of the flat surface of the sample. There will be no  $\theta$  dependence of any variables, and no displacement in the  $\theta$  direction. The saucer is taken to be a segment of a sphere, of depth  $h$  and radius  $b$  in the plane  $z = 0$ , so in fact the saucer region is defined by  $z \leq 0$  for the flat surface, and  $r^2 \leq (z+h)(b^2/h-z)$  for the spherical cap. The equilibrium position of the needle is taken to be the cylinder  $r \leq a, z \geq -h_1$ . We also define  $h_2$  to be the depth of sample below the needle, so  $h = h_1 + h_2$ .

During the motion, the needle has a vertical displacement which we denote by  $s(t)$ . For our small strain assumption to be valid we require that  $|s| \ll h_2$ , since the maximum strain will occur where the moving needle is closest to the fixed base, *i.e.* in the region immediately beneath the needle.

If we let  $\mathbf{u}(\mathbf{x}, t)$  denote the displacement field within the sample, then the assumptions that the base and needle are rigid give us

$$\mathbf{u} = (0, 0, 0) \quad \text{on the base,} \quad \mathbf{u} = (0, 0, s) \quad \text{on the needle.} \quad (1)$$

On the free surface ( $z = 0, a < r < b$ ) there is no prescribed displacement, but there is no applied stress, so with  $\sigma$  as the stress tensor we have

$$\sigma_{zz} = 0, \quad \sigma_{rz} = 0 \quad \text{on the free surface.} \quad (2)$$

### 3.2 Modelling the viscoelasticity of the sample

We here summarize the standard linear theory of viscoelasticity, and the associated terminology, as found in for instance Pipkin's book [3].

As we have already seen, it is reasonable to assume that the sample only deforms in shear, and to begin with we think of a cuboid of material being deformed in simple shear as in Figure 2. For a linear purely elastic solid there is a relationship  $\sigma = G\gamma$  between the

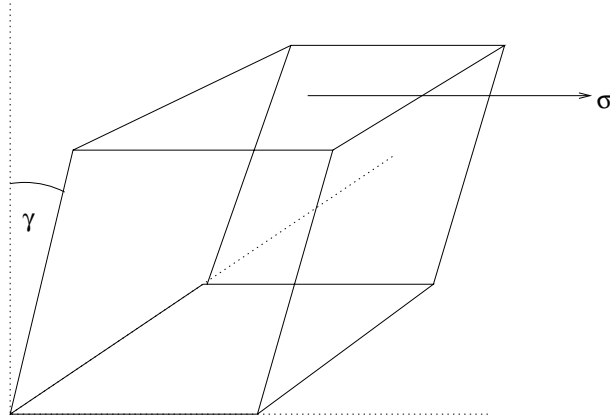


Figure 2: Shear stress  $\sigma$  and shear angle  $\gamma$

instantaneous values of the shear stress  $\sigma$  and the shear angle  $\gamma$ , which defines the shear modulus  $G$ . For a Newtonian viscous fluid, there is a linear relation between  $\sigma$  and the

rate of shear,  $\sigma = \eta\dot{\gamma}$ , which defines the dynamic viscosity  $\eta$ . For a general viscoelastic material, the shear angle  $\gamma$  depends on the past history of  $\sigma$ , and if this dependence is linear then we can write

$$\gamma(t) = \int_0^\infty c(\tau)\sigma(t-\tau) d\tau. \quad (3)$$

If  $\sigma$  varies sinusoidally, then (after any transient behaviour has decayed)  $\gamma$  will also vary sinusoidally. We make the convention that we shall then write  $\sigma(t) = \Re(\sigma_c e^{i\omega t})$  so  $\sigma_c$  is the complex amplitude, and  $\omega$  denotes the *radian* frequency, so  $\omega = 2\pi f$  if  $f$  is measured in Hertz. We then have

$$\gamma_c = C(\omega)\sigma_c, \quad C(\omega) = \int_0^\infty c(\tau)e^{-i\omega\tau} d\tau. \quad (4)$$

This  $C(\omega)$  is called the *shear compliance*, and its reciprocal is the *dynamic shear modulus*  $G(\omega)$ , with real and imaginary parts  $G'$ ,  $G''$ , so

$$\sigma_c/\gamma_c = 1/C(\omega) = G(\omega) = G'(\omega) + iG''(\omega).^1 \quad (5)$$

$G'(\omega)$  is known as the *storage modulus*,  $G''(\omega) \geq 0$  is the *loss modulus*, and  $\tan \delta = \arg(G) = G''/G'$  is the *loss tangent*. The static value  $G(0) = G_e$  is real and called the *equilibrium modulus*. The high frequency limit  $\lim_{\omega \rightarrow \infty} G(\omega) = G_g \geq G_e$  is real and called the *glassy modulus*. The storage and loss moduli are related by the Kramers-Kronig relations, expressing the fact that the material responds causally:

$$G''(\omega_1) = \frac{1}{\pi} P \int_{-\infty}^{\infty} \frac{G'(\omega) - G_g}{\omega - \omega_1} d\omega, \quad G'(\omega_1) = G_g - \frac{1}{\pi} P \int_{-\infty}^{\infty} \frac{G''(\omega)}{\omega - \omega_1} d\omega, \quad (6)$$

where  $Pf$  denotes the Cauchy principal value of the integral.

For a purely elastic solid,  $G$  is real and independent of frequency. For a Newtonian viscous fluid,  $\sigma = \eta\dot{\gamma}$ , and so  $G(\omega) = i\omega\eta$ , where  $\eta$  is the dynamic viscosity. A general model for a viscoelastic material that includes both these limits as special cases is the ‘standard linear solid’ or Maxwell-Voigt model, in which  $\sigma$  and  $\gamma$  are related by

$$\sigma + T\dot{\sigma} = G_e\gamma + G_g T\dot{\gamma}, \quad (7)$$

with a relaxation time  $T > 0$  in addition to the parameters  $G_e$ ,  $G_g$  already introduced. This then gives

$$\frac{\sigma_c}{\gamma_c} = \frac{G_e + G_g i\omega T}{1 + i\omega T} = G(\omega) = G'(\omega) + iG''(\omega), \quad (8)$$

from which the real and imaginary parts  $G'$ ,  $G''$  can easily be separated out.

These relationships are for simple shear, and to generalize them to the appropriate tensor form for an incompressible material we shall have a displacement field  $\mathbf{u}(\mathbf{x}, t)$  with strain tensor

$$e_{ij} = \frac{1}{2} \left( \frac{\partial u_i}{\partial x_j} + \frac{\partial u_j}{\partial x_i} \right), \quad (9)$$

---

<sup>1</sup>The terminology is standard. Note that  $G'$  and  $G''$  are *not* the first and second derivatives of  $G(\omega)$  with respect to  $\omega$ .

(in Cartesian coordinates). Incompressibility is represented by

$$\text{Tr}(e) = \sum_i \frac{\partial u_i}{\partial x_i} = 0, \quad (10)$$

and the stress tensor  $\sigma_{ij}$  is given by

$$\sigma_{ij} + T\dot{\sigma}_{ij} = -p\delta_{ij} + 2(G_e e_{ij} + G_g T\dot{e}_{ij}), \quad (11)$$

so  $p$  is analogous to hydrostatic pressure. (The factor of 2 arises because for simple shear in the  $i, j$  plane,  $e_{ij} = \gamma/2$ .) Alternatively, if  $\sigma$ ,  $p$ , and  $\mathbf{u}$  are varying sinusoidally and we express them in terms of complex amplitudes  $\sigma_c$ ,  $p_c$  etc, then

$$(\sigma_c)_{ij} = -p_c\delta_{ij} + 2G(\omega)(e_c)_{ij}. \quad (12)$$

These models are just as discussed in p93–95 of [3].

## 4 Modelling the vibrator

We adopt a simplified model of the vibrator, in which the relevant effects are:

- A linear relationship between the force  $F$  that the vibrator applies to the needle assembly, and the current  $I$  flowing through the coil,

$$F = KI. \quad (13)$$

- A simple  $LR$  circuit for the current in the coil

$$V = IR + L\dot{I} + V_b \quad (14)$$

where  $V$  is the applied alternating electromotive force,  $R$  and  $L$  are the resistance and inductance of the circuit, and  $V_b$  is the back emf in the coil.

- Simple proportionality between the back emf and the needle velocity

$$V_b = K\dot{s}. \quad (15)$$

This is just the Faraday effect, and in a simple linear model like this, reciprocity makes this constant  $K$  the same as in (13).

- We assume the damping and elastic forces on the needle due to its mounting are  $\lambda\dot{s}$  and  $k_0s$  for constants  $\lambda$ ,  $k_0$ .

The equation of motion of the needle then is

$$F = m\ddot{s} + \lambda\dot{s} + k_0s + F_s \quad (16)$$

where the first three terms are the inertia, and the damping and elastic forces, and  $F_s$  is the force applied by the needle to the sample. The vibrating mass is  $m = m_n + m_v$  where  $m_n$  is the mass of the needle and the pin vice that holds it, and  $m_v$  is the mass of

the vibrating part of the mechanism itself — the coil and some fraction of the mounting etc. For sinusoidal driving, we write  $F = \Re(F_c e^{i\omega t})$  as usual, and the complex amplitude of the back emf is then

$$(V_b)_c(\omega) = \frac{KF_c}{mi\omega + \lambda + k_0/(i\omega) + Z_s(\omega)}, \quad (17)$$

where  $Z_s(\omega)$  is the mechanical impedance of the sample

$$Z_s(\omega) = (F_s)_c/(\dot{s})_c. \quad (18)$$

For a constant thrust vibrator,  $F_c$  is independent of frequency, so the measured amplitude of the back emf depends on the sample through this impedance  $Z_s(\omega)$  in the denominator of (17). The resonant frequency  $\omega_r$  and peak amplitude  $|V_b|_{\text{res}}$  then are given by

$$|V_b|_{\text{res}} = |(V_b)_c(\omega_r)| = \max_{\omega} |(V_b)_c(\omega)|, \quad (19)$$

and the measured resonant frequency in Hz is  $f_r = \omega_r/(2\pi)$ .

## 5 Sample impedance

If we were to write down the full dynamic equations for the motion of the sample, we would have (in Cartesians)

$$\sum_j \frac{\partial \sigma_{ij}}{\partial x_j} = \rho \frac{\partial^2 u_i}{\partial t^2}, \quad (i = 1, 2, 3). \quad (20)$$

The smallest terms on the left are of order  $|G||s|/b^2$ , whereas on the right we have terms of order  $\rho\omega^2|s|$ . The ratio of these is

$$\frac{\rho\omega^2|s|}{|G||s|/b^2} = \frac{\rho\omega^2 b^2}{|G|}. \quad (21)$$

For typical sample properties and dimensions, we have

$$\begin{aligned} \rho &\approx 10^3 \text{ kg/m}^3, & G &\approx 2 \times 10^5 \text{ N/m}^2, & b &\approx 6 \text{ mm} = 6 \times 10^{-3} \text{ m}, \\ \omega &= 2\pi f, & f &\approx 170 \text{ Hz}. \end{aligned} \quad (22)$$

This makes the parameter above about 0.2. This suggests the next main approximation we make, which is to neglect the inertial terms in (20) and so replace it by the quasistatic equation

$$\sum_j \frac{\partial \sigma_{ij}}{\partial x_j} = 0, \quad (i = 1, 2, 3). \quad (23)$$

An equivalent way of stating this assumption is to say that we are ignoring all effects of elastic wave propagation in the sample, on the grounds that its maximum dimension  $b$  is small compared to the elastic wavelength at the frequency of operation. Yet another way of stating it is to say that the mass of the sample is small compared with the mass of the needle.

## 5.1 Scaling

We shall now nondimensionalize the problem and introduce dimensionless coordinates  $\hat{\mathbf{x}} = \mathbf{x}/a$ , with displacements  $\hat{\mathbf{u}}(\hat{\mathbf{x}}) = \mathbf{u}_c(\mathbf{x})/s_c$ , pressure  $\hat{p} = p_c/(G(\omega)s_c/a)$ , and stresses  $\hat{\sigma}_{ij} = (\sigma_c)_{ij}/(G(\omega)s_c/a)$ . The dimensions of the saucer then are given by  $B = b/a$ ,  $H = h/a$ , the needle contact length is  $H_1 = h_1/a$ , and the clearance below it is  $H_2 = h_2/a$ . The dimensionless problem then is

$$\sum_i \frac{\partial \hat{u}_i}{\partial \hat{x}_i} = 0, \quad \hat{\sigma}_{ij} = -\hat{p}\delta_{ij} + \frac{\partial \hat{u}_i}{\partial \hat{x}_j} + \frac{\partial \hat{u}_j}{\partial \hat{x}_i}, \quad \sum_j \frac{\partial \hat{\sigma}_{ij}}{\partial \hat{x}_j} = 0, \quad (24)$$

with boundary conditions

$$\begin{aligned} \hat{u} &= (0, 0, 0) && \text{on the base,} \\ \hat{u} &= (0, 0, 1) && \text{on the needle,} \\ \hat{\sigma}_{3i} &= 0 && \text{on the free surface.} \end{aligned} \quad (25)$$

The dimensionless force that the needle applies to the sample then is

$$N = \int_{\text{needle}} \hat{\sigma}_{3i} n_i dA \quad (26)$$

where  $\mathbf{n}$  is the unit normal vector on the needle surface, (directed sample  $\rightarrow$  needle). This constant  $N$ , dependent on the shape of the sample, is the crucial calibration constant of the equipment, and the mechanical impedance is given in terms of it by

$$Z_s(\omega) = \frac{NG(\omega)a}{i\omega} \quad (27)$$

The best method for calculating  $N$  numerically would be by a finite element method, either formulating the problem along the lines outlined in [2], or using a stress function as in §188 of Love [4]. It is planned that an Oxford MSc student, Philipp Funke, will work on this.

Alternatively, calibration of the geometry with an incompressible material of *known* shear modulus would also provide the value — though if one were designing a device with a new geometry then a numerical procedure avoids the need to build a prototype.

## 5.2 Bounds for the calibration constant<sup>2</sup>

At the Study Group, the numerical computation of  $N$  was not attempted, but it is possible to produce bounds on  $N$  by solving related problems that have sufficiently simple geometry to allow exact solution. One example already mentioned in [2] is the comparison with the Hertz indenter problem ( $H_1=0$  and  $B, H \rightarrow \infty$ ) which guarantees  $N > 8$ . The Study Group obtained the bound

$$N > \frac{2\pi H_1}{\log B - (B^2 - 1)/(B^2 + 1)} + \frac{3\pi}{H_2}, \quad (28)$$

---

<sup>2</sup>Note: Philipp Funke has pointed out (July 2001) that the analysis of this section 5.2 is incorrect, and does not prove that the given expressions are bounds on the calibration constant: the reason is that the cylindrical annulus of material introduced has non-zero shear stresses on its flat surfaces. The reader may therefore prefer to skip this section (or provide a correct analysis).

and for the dimensions of the geometry supplied by RAPRA this gives  $N > 18.6$ . ( $a = 0.75$  mm,  $b = 6$  mm,  $h_1 = 2$  mm,  $h_2 = 2$  mm; so  $B = 8$ ,  $H_1 = H_2 = 8/3$ .) As will be seen from the derivation below, this is a fairly crude lower bound, not intended to be a good estimate. However, the fact that it is well over 8 shows that the geometry of the sample is giving it a considerably greater stiffness than the Hertz indenter problem.

The bound (28) is obtained by considering the situation shown in Figure 3, where the sample occupies a solid cylindrical annulus around the needle, and a cylinder below the needle, and the rest of the “saucer” is filled with incompressible fluid. This configuration

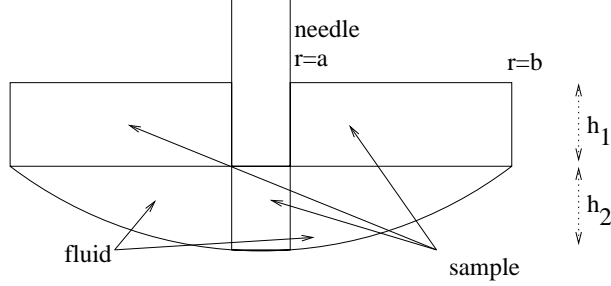


Figure 3: Configuration yielding lower bound (28)

has consistently replaced materials by materials of lower shear modulus — part of the steel (treated as rigid) by the sample material, and part of the sample material by an incompressible fluid (zero shear modulus) — so it has certainly *decreased* the stiffness of the system. Hence if we can calculate the stiffness of this then we have a *lower* bound on  $N$ .

It is easiest to compute the stiffness in stages. First, if we simply had an annulus of material,  $-h_1 \leq z \leq 0$ ,  $a \leq r \leq b$ , of thickness  $h_1$  and inner and outer radii  $a$  and  $b$ , then when it is deformed by an axial displacement  $s$  of the inner boundary  $r = a$ , and is in equilibrium with an axial force  $F_s$ , the shear stress is  $\sigma_{rz} = -F_s/(2\pi r h_1)$ , so the axial displacement  $w$  obeys  $dw/dr = 2e_{rz} = -F_s/(2\pi r h_1 G)$ . Thus  $w = F_s \log(b/r)/(2\pi h_1 G)$ , where we have chosen the constant of integration to make  $w = 0$  at  $r = b$ . Hence the displacement of the needle is  $s = w(a) = F_s \log(b/a)/(2\pi h_1 G)$ . So the stiffness of this configuration is  $2\pi h_1 G / \log(b/a)$ , or  $2\pi H_1 / \log B$  in dimensionless terms.

Now, if such an annulus is constrained below by a fixed volume of incompressible fluid, then a hydrostatic pressure  $p$  will arise in the fluid. Thus the equilibrium shear stress will now be  $\sigma_{rz} = -(F_s + \pi r^2 p)/(2\pi r h_1)$ , so  $dw/dr = -(F_s + \pi r^2 p)/(2\pi r h_1 G)$ , and  $w(r) = (F_s \log(b/r) + \pi p(b^2 - r^2)/2)/(2\pi h_1 G)$ , where we have again chosen the constant of integration to make  $w = 0$  at  $r = b$ . The value of  $p$  is now fixed by the constraint that the volume of fluid below the annulus is constant, so  $\int_a^b w(r) 2\pi r dr + \pi a^2 w(a) = 0$ . This gives  $p = -2F_s/(\pi(b^2 + a^2))$  and so the needle displacement can be found as

$$s = w(a) = F_s(\log(b/a) - (b^2 - a^2)/(b^2 + a^2))/(2\pi h_1 G). \quad (29)$$

So the stiffness of this configuration is  $2\pi h_1 G / (\log(b/a) - (b^2 - a^2)/(b^2 + a^2))$ , which is of course greater than that without the fluid. In dimensionless terms, this stiffness is  $2\pi H_1 / (\log B - (B^2 - 1)/(B^2 + 1))$  and it provides the first term in (28).

If we now add in the cylinder of incompressible material below the needle, then its stiffness, just considered as a rod of length  $h_2$ , area  $\pi a^2$ , and Young’s modulus  $E = 3G$

would be  $3G\pi a^2/h_2$ . In dimensionless terms, this is  $3\pi/H_2$ , the second term in (28). Two notes on this are in order:

1. The value  $3G\pi a^2/h_2$  assumes that the ends of the rod are free to move radially in response to Poisson's ratio effects. If the ends are in fact constrained not to move radially, that will further increase the stiffness, so (28) will hold *a fortiori*;
2. The hydrostatic pressure  $p$  calculated previously can of course be superimposed on the pressure field calculated for the stretched incompressible rod without any effect, so their contributions to the stiffness can simply be added.

## 6 Analysis of model

Going back to physical variables, the complex amplitudes of  $F_s$  and  $s$  are related by

$$(F_s)_c = NG(\omega)as_c, \quad (30)$$

so for a viscous fluid,  $F_s = N\eta a\dot{s}$ , while for an elastic solid,  $F_s = NGas$ . It is the same numerical constant  $N$  that occurs in both these cases. In general,

$$Z_s = \frac{(F_s)_c}{(\dot{s})_c} = \frac{NGa}{i\omega} = \frac{NG''a}{\omega} + \frac{NG'a}{i\omega}. \quad (31)$$

Substituting this into the result (17) earlier we see

$$(V_b)_c = \frac{KF_c}{mi\omega + (\lambda + NG''a/\omega) + (k_0 + NG'a)/(i\omega)}. \quad (32)$$

This shows quantitatively the effects we expect: the real part  $G'$  of  $G$  contributes to the elastic stiffness, raising it from the value  $k_0$  inherent in the vibrator to  $k_0 + NG'a$ ; and the imaginary part  $G''$  of  $g$  contributes to the damping constant, raising it from the value  $\lambda$  inherent in the vibrator to  $\lambda + NG''a/\omega$ . We shall now comment on this result in various cases for which RAPRA have provided details.

### 6.1 Viscous fluids

RAPRA have conducted experiments in which a variety of viscous fluids are used as the sample. If the fluid is Newtonian with dynamic viscosity  $\eta$ , then  $G'(\omega) = 0$  and  $G''(\omega) = \omega\eta$  and so

$$(V_b)_c = \frac{KF_c}{mi\omega + (\lambda + N\eta a) + k_0/(i\omega)}. \quad (33)$$

Thus we can deduce that

- the resonant frequency is at  $\omega = \omega^* = \sqrt{k_0/m}$ , whatever the viscosity;
- at a given frequency  $\omega$  the amplitude of response  $|(V_b)_c|$  should decrease as the viscosity  $\eta$  increases;

- the peak (resonant) amplitude

$$|V_b|_{\text{res}} = \frac{KF_c}{\lambda + N\eta a} \quad (34)$$

should decrease with viscosity;

- a plot of  $|V_b|_{\text{res}}^{-1}$  against viscosity  $\eta$  should be a straight line.

In the experimental data provided by RAPRA in [1], the first of these conclusions holds quite accurately: the data summarized on the page ‘SVNC resonance peaks for different damping media’ show a resonance frequency of 43–45 Hz for air, a 30 Pa s silicone, Golden syrup, and cane sugar at 122° C. The same page shows that the second conclusion was valid at frequencies from 30–65 Hz (a broad band around the resonance), but failed outside that range. Above 65 Hz the response in air fell below that in the silicone, while below 30 Hz the response in cane sugar rose above that in Golden Syrup, then above the other 2 as well. Neither the Study Group nor BW could offer any explanation of this.<sup>3</sup> The third conclusion was very evidently satisfied in the RAPRA data, both on the page referred to and on the page ‘Amplitude and Viscosity’. The fourth conclusion did not hold however — when the data points on this last plot were read off and reciprocal voltages plotted, the five points formed a concave curve not a straight line. Again, the reason for this is unknown.

## 6.2 Elastic solids

If the sample is purely elastic then we have  $G'' = 0$  and  $G' = G$ , so

$$(V_b)_c = \frac{KF_c}{mi\omega + \lambda + (k_0 + NGa)/(i\omega)} \quad (35)$$

so the resonant frequency  $\omega_r$  is given by

$$\omega_r^2 = (k_0 + NGa)/m, \quad (36)$$

and the resonant amplitude is

$$|V_b|_{\text{res}} = KF_c/\lambda. \quad (37)$$

This suggests the idea of plotting  $\omega_r^2$  against  $G$  for a variety of elastic materials and seeing if a straight line results. Rather than this, RAPRA have plotted  $\omega_r^2$  during a cure against the value of  $G'(\omega_1) = \Re(G(\omega_1))$  measured in a conventional oscillating rheometer for the same cure. (This was a polyurethane cast elastomer, curing at 40° C.) If we attempt to generalize (36) to the case of a viscoelastic material we would predict a resonant frequency  $\omega_r$  determined approximately by

$$\omega_r^2 = (k_0 + NG'(\omega_r)a)/m. \quad (38)$$

---

<sup>3</sup>Andrew Lacey suggests it may be an artifact of just what voltage is measured, and that this could happen if the amplitude of the applied voltage is used. This depends on the details of what happens in the vibrator electronics to produce the given output signal, much of which we do not know.

This is obtained simply by making the imaginary part of the denominator of (32) vanish. In fact this will only give the exact maximum of  $|(V_b)_c|$  if  $G''(\omega)/\omega$  is constant (as occurs for a viscous fluid or an elastic solid). We shall mention later how the damping will affect this, but for the moment we continue with this approximation. To get a straight line on the basis of this we should obviously plot  $\omega_r^2$  against  $G'(\omega_r)$ , but in fact the oscillating rheometer was operated at a fixed frequency of 1 Hz, so  $\omega_1 = 2\pi$ , and  $\omega_r^2$  was plotted against  $G'(\omega_1)$ . This graph (included in [1]) showed a straight main section where  $G'$  was rising from about  $3 \times 10^4$  Pa to  $19 \times 10^4$  Pa, with deviations at the beginning and end of the cure. In the initial stages, where  $G' < 3 \times 10^4$  Pa, the sample is still quite liquid, and we would not expect the elastic relation to hold. In the final stages, where  $G' > 19 \times 10^4$  Pa, RAPRA is not certain that the values of  $G'$  measured by the oscillating rheometer are reliable. Over the straight section, RAPRA fit the straight line as  $f_r^2 = 12875 + 0.0655G'$  when  $f_r$  is the resonant frequency in Hz. Comparing this with the elastic result, we have

$$\frac{Na}{m} = 0.0655(2\pi)^2, \quad (39)$$

and with  $a = 0.75$  mm, and  $m = m_n + m_v$  with the needle mass  $m_n = 11.56$  g (including the pin vice and the vibrator mass  $m_v = 7.15$  g, this gives  $N \approx 64.5$ . As expected, this is considerably in excess of the lower bound 18.6 derived earlier. However, there is of course the question whether  $G'$  varies significantly between  $\omega_1$  (1 Hz) and  $\omega_r$  (75 to 170 Hz). We discuss this below.

A further comment here is that RAPRA [1] quote a value  $k_0 = 106.2$  N/m, and for the needle vibrating in air this would give resonance at  $\omega_r = \sqrt{k_0/(m_n + m_v)} = 75.34$  rad/s, so  $f_r = \omega_r/(2\pi) = 12$  Hz. This is too low, and we do not understand what has happened here — whether perhaps factors of  $2\pi$  have gone astray in extracting the value of  $k_0$  from the measurements?

### 6.3 Viscoelastic materials

When the material is a standard linear solid (7), then the resonant frequency will be given approximately by (38), but more exactly by the maximization in (19). Various questions then arise:

1. The values of the equilibrium modulus  $G_e$ , the glassy modulus  $G_g$ , and the relaxation time  $T$  are *all* varying during the cure. We cannot hope to extract instantaneous values of *all* of them by measuring just resonant frequency and amplitude. A crucial question is whether the relaxation frequency  $1/T$  of the material lies in or passes through the resonant range (say 75–170 Hz) during the cure. When  $\omega_r T \gg 1$ , the SVNC is measuring the glassy modulus, and when  $\omega_r T \ll 1$  it is measuring the equilibrium modulus, but without some *a priori* knowledge of the relaxation time in the material we cannot know which stages of the cure lie at or between these extremes.
2. A further point is that in a chemically reacting material, we cannot really measure its *long-time* behaviour. We can believe it has a high frequency glassy modulus  $G_g$ , and that  $G(\omega)$  is defined for frequencies  $\omega$  that are sufficiently large compared with the reaction rate, but not below that.

## 7 RAPRA's questions

We just outline the answers that this approach suggests to the questions posed by RAPRA.

1. *Should  $\omega_r^2$  be plotted against  $G'(\omega_r)$ , or at least against  $G'(\omega_t)$  for some frequency  $\omega_t$  more typical of  $\omega_r$ ?*  
(This refers to getting the graph with a straight section mentioned in 6.2.) Ideally, yes: but if it were known *a priori* that the variation of  $G'$  from DC to 200 Hz is small, then it would not matter much.
2. *Would an easier sample geometry be better?*  
A different sample geometry might make the calculation of the calibration constant more tractable analytically, but this is not a big problem. For any sample geometry the calibration constant  $N$  can be found either by doing just one finite element calculation, or by building a prototype and testing with an incompressible material of known shear modulus. In numerical terms, once a suitable finite element code is written, or suitable freeware code located, to do incompressible axisymmetric elastostatics, that is enough.
3. *Can we measure  $G'$  at other frequencies?*  
No: the SVNC just sees  $G'(\omega_r)$  and checks that it produces a local maximum of the amplitude. Deducing behaviour at other frequencies would depend on having some *a priori* knowledge of the material relaxation time.
4. *Can we derive other material properties?*  
Not directly: only if they are empirically correlated with  $G$ .

### 7.1 Suggestions

Some suggestions were made for how further information might be obtained from the SVNC:

1. Can the vibrator electronics measure phase information? If the relative phase between  $V_b$  and the applied force  $F$  were known, that obviously would provide additional information that is lost when just the modulus is taken. How valuable this would be depends on how much viscous loss occurs in the material, which in turn depends on the question raised earlier about relaxation times.
2. After the material has set, can the SVNC scan over frequency to produce a plot of  $V_b$  against frequency for the *cured* material? This would presumably enable the SVNC to give useful information about the cured material without much extra work, and for the material sample in exactly the same geometry that is used during the curing measurements.
3. Would white noise forcing be better than sinusoidal? The idea here would be to use band-limited white noise, to excite the sample over a whole band of frequencies simultaneously, and measure the spectrum of its response. Effectively, one would

be trying to measure the whole function  $V_b(\omega)$  at each stage of the cure, rather than just the position of its peak.

## References

- [1] The Scanning Vibrating Needle Curemeter (SVNC). RAPRA Technology Ltd. Problem description for ESGI2001, Keele, April 9-12 2001.
- [2] Notes on SVNC workshop. OCIAM workshop report, 17-Nov-2000.
- [3] Lectures on Viscoelasticity Theory. A C Pipkin. Springer-Verlag, New York, 1972.
- [4] A Treatise on the Mathematical Theory of Elasticity. A E H Love. 4th ed, CUP, 1927. Reprinted by Dover, New York.